Impact of Aluminium on ZnO Thin Films for Antimicrobial Activity

BA ANANDH (anandh.ba@gmail.com)
PSG College of Arts and Science https://orcid.org/0000-0001-9825-4794
R SAKTHIVEL
A SHANKAR GANESH
S SUBRAMANI
A T RAJAMANICKAM

Research Article

Keywords: Al doped ZnO, XRD, Hexagonal Wurtzite Structure, FESEM, UV-Vis, PL, Antibacterial activity, Antifungal activity

Posted Date: May 13th, 2021

DOI: https://doi.org/10.21203/rs.3.rs-518844/v1

Version of Record: A version of this preprint was published at Asian Journal of Chemistry on September 24th, 2021. See the published version at https://doi.org/10.14233/ajchem.2021.23342.

Abstract

Thin films of pure Zinc Oxide (ZnO) and Aluminium (Al) doped ZnO were deposited by two step SILAR technique. Pure and Al (1%, 3%, 5%) doped ZnO thin film's structural, morphology and optical properties were analyzed. Diffraction peaks of the all the samples were indexed to hexagonal wurtizite structure. The crystallite size, lattice parameters, dislocation density and microstrain were calculated for the prepared thin films. Morphology study using FESEM shows spherical shaped structure of pure ZnO and hexagonal faced rod like structure for Al doped ZnO thin films.T he UV-Vis absorption spectrum for the thin films was also studied. There is decrease in bandgap as the Al doping ratio increases from 1–5%. Photoluminescence (PL) studies confirm that oxygen ion vacancy and interstitial Zn^{+} ion were present. The maximum zone of inhibition was studied against the bacteria's the Gram-negative (E.coli) and Gram-positive (S.aureus) by Agar diffusion method. Significant antibacterial result was seen in pure and Al doped ZnO. Al doped ZnO shows more antibacterial activity over pure ZnO. All the samples give considerable antifungal activity which was done against Aspergillusniger.

.

1. Introduction

Zinc oxide (ZnO) is a semiconductor with possible applications in different fields because of its significant physical properties. It is an II-VI semiconductor which crystallizes in rock salt, wurtzite and rock salt forms. ZnO is more stable in the hexagonal wurtzite phase rather than other phases at room temperature. Studies on thin films have improved several novelparts of analysis which depends on exclusive characteristic and structures [1]. ZnO has very good chemical stability, excellent thermal stability, high exciting binding energy (60meV) and wide bandgap (3.37eV) at room temperature. ZnO thin films have good electrical and optical properties, very high electrical resistivity, low cost and are non-toxic [2].

The inorganic compound ZnO has very good resistance against microorganisms [3]. ZnO is an important material for preventing the influenceof food pathogens such as Staphylococcus aureus (S.aureus) and Escherichia coli (E.coli) on the food items [4]. It is also useful in skin treating products like ointments, diaper rashes, baby powder, etc. ZnO also has good antifungal activity [5] which is used for protecting the wood from fungal activity [6]

Pure ZnO films are found to unstable because of chemisorptions and adsorption that modifies the surface conductance [7]. By adding anionic and cationic dopant such as Cu, Sn, Mn, Ag, Fe, Mg and Al, the properties of Zinc Oxide can be modified and the thin films greatly conductive which could be the other options for cheaper transparent conducting layers for various applications like anti-bacterial, antifungal, gas sensing, photocatalytic properties and solar cell [8–11] etc. Among the dopants Aluminum is one of the best dopant to get thin films of both transparent and conductive in the visible region. So, it can be used in transparent conductive composites. Currently, preparation of thin films has

number of deposition techniques like dip coating, sputtering, chemical bath deposition, spray pyrolysis, sol-gel deposition and Successive Ionic Layer Adsorption and Reaction (SILAR) [12–17]. Among these, SILAR is one of the commonly used techniques for preparing thin films because of its ease, inexpensive, non-vacuum technique and even coating over a larger area.

The aim of the present study is to prepare pure and Al doped ZnO thin films by SILAR technique and to investigate the structural, surface morphology and optical property for the prepared films. Also to analyze the antibacterial and antifungal activity, since there are few studies for Al doped ZnO thin films and merely no studies available for Al doped ZnO thin films prepared by SILAR techniques.

2. Experimental Procedure

Glass slide is taken as substrate for depositing pure and Al doped ZnO thin films by SILAR technique. Zinc acetate dehydrates (ZAD) and aluminium acetate was used as source and dopant material for preparing the thin films,. 0.1M of precursor (ZAD) was dissolved in 100ml of solvent (ethanol). Monoethanolamine (MEA) is added drop by drop to obtain clear and uniform zincate solution. The zincate solutions are prepared for pure ZnO, 1%, 3% and 5% Al doped content. Film deposition was carried out by dipping the pre-cleaned microscopic glass substrate alternatively in zincate bath which is kept at room temperature and hot deionised water bath which is kept between 90ºC to 100ºC. One set of dipping involves 30 second dipping in zincate bath and in a hot deionised water bath. This process was repeated for 30 cycles to obtain the thin film and the film is post annealed at 250ºC.

Assessment of Antibacterial Activity

E.coli (Gram negative) and S.aureus (Gram positive) bacteria's were used for assessing the antibacterial activity of the prepared pure and Al doped ZnO. Agar diffusion method is used for assessing the antibacterial activity. Sterile Muller Hinton (MHA) agar was distributed within sterile petri dishes. The culture specimen was adjusted to 10^8 cfu/ml. The surface of the agar plate was swabbed over using sterile cotton swab. Prepared samples were kept at the middle of the plate **and pressed softly** and were incubated for 24 hours at 37^{o}C. The incubated plates were then tested for the interruption of growth sample. The diameter of the inhibited growth near the sample was measured to find the zone of inhibition.

Assessment of Antifungal Activity

Agar diffusion method is used for the antifungal activity on ZnO and Al doped ZnO. The antifungal assessment used Potato dextrose agar medium and Aspergillus niger was the test organism. A petridish was dispensed with the prepared potato dextrose agar medium and the spores of fungi have been inoculated into sterile distilled water having few glass beads and shaken energetically to take the spores into suspension. The surface of the agar was diffused uniformly with 1.0 ± 0.1 ml of inoculums. The test samples were set in agar medium and they were incubated at 27°C. The zone of mycosis under and along the sides of the samples was measured after the incubation period. The incubated plates were inspected

for interruption in the growth of inoculums. The size of the clear region was noted for assessment of the inhibitory impact of the assessment sample.

3. Result And Discussion

3.1 Structural Analysis

Fig. 1(a) indicates the X-ray diffraction patterns of pure and Aluminium doped ZnO films annealed at 250ºC. The diffraction peaks observed at (100), (002), (101), (102), (110), (103), (200), (112), (201), (004) and (202) lattice plane confirms hexagonal Wurtzite structure of the prepared films as it well matches with the JCPDS card number 36-1451. The film pattern with the highest intensity at the (002) plane reveals the orientation of the particles are along the c-axis. This may be owing to the negligible interior stress and surface energy and also because of the high atomic density that makes the crystallites grow towards the c-axis easily [18, 19]. The right shift was observed in the main peak position which is shown in fig. 1(b). The doped samples illustrate that the planes (100), (002) and (101) exhibits a shift towards the higher angle side. This shift observed in the peak is owing to the attribution of ionic radii of the dopant Al^{3+} ion which is small when compare to Zn^{2+} ion. The Peaks also found to broaden with the increase in Al concentration.

Table1 Structural parameters of pure, 1%, 3% and 5% Al doped ZnO thin films

Thin film Sample	Crystallite Size (D) nm	Microstrain (ε) x 10^{-3}	Dislocation Density (δ) x10^{15}lines/m^2	Unit Cell volume $(Å)^3$	Lattice constants(Å)	
A	c					
Pure ZnO	30.05	1.2054	1.1085	47.6139	3.2492	5.2075
1 % Al	19.27	1.8793	2.6944	47.1123	3.2391	5.1848
3 % Al	19.31	1.8756	2.6837	47.0456	3.2381	5.1808
5 % Al	18.40	1.9685	2.9562	47.1342	3.2406	5.1825

Various structural parameters of pure and Al doped ZnO thin films are shown in Table 1. The crystallite size of the prepared films is calculated using Debye-Scherrer's formula. Table 1 clearly shows that, there is a decrease in the crystallite size of Al doped thin film when comparing with pure ZnO thin film. It may be because of large number of dislocations and stress created by the ionic radii from Al ions that take up the interstitial sites within the ZnO crystal lattice [20]. Lattice constants for the prepared films are well matched with the standard values. The lattice constant 'a' and 'c' are smaller in Al doped thin films than that of pure ZnO thin film. Incorporation of Al ion into Zn ion leads to compression of lattice because Al^{3+} ion is small than that of Zn^{2+} ion. Obtained crystallite size and the microstrain indicate that they are

sensitive to Al doping. In addition, Fig. 2 shows the changes of the crystallite size along with the microstrain as a function of Al ratio, showing the likely reduction in the crystallite size which may be seen from the diffraction peak broadening as shown in fig. (1b). The Dislocation density of pure ZnO thin film is 1.1085 x 10^{15} lines/m^2 and is increased to 2.9562 x 10^{15}lines/m^2 after Al doping. These results highlight that there is an increase in lattice imperfection in the Al doped ZnO thin film.

3.2 Surface Morphology

Fig.3 illustrates the Field Emission Scanning Electron Microscope (FESEM) images of Al doped and pure ZnO thin films. Spherical shaped particles are seen in pure ZnO thin film fig.3 (a). FESEM images of Al doped ZnO thin films are shown in Fig.3 (b) – (d). Al doping influences large change in the grains and modification of spherical shape to hexagonal faced rod like structure. This shape is random in alignment for 1% Al doped ZnO and when the concentration is further increased to 3% and 5% they exhibit the agglomeration in grains and almost covers the entire substrate surface with rod like structure. Such changes in the shape of particles is owing to the formation of quantum properties on the surface and opposite effect of oxide formation of Al-O-Zn [21]. The images clearly indicate that the average crystallite size is decreased with increasing the Al concentration. Hence it can be presumed that Al doping have a vital part in controlling the morphology of the films.

Fig. 4 (a) – (d) indicates the Atomic Force Microscopy (AFM) graphs for pure and Al doped (1%, 3% and 5%) ZnO thin films with a scanning area of 3x3 micro meter. The surface property for 1%, 3% and 5% Al doped ZnO thin films seems to be thick and are good quality films. The pure ZnO have smooth surface and the surface roughness seems to increase with increase in Al content. The Root mean square (RMS) values of films with pure, 1%, 3% and 5% Al concentration are 10.76, 23.87, 34.96 and 44.29 respectively. The average roughness is found to be 5.46, 15.99, 26.30 and 32.98 for pure, 1%, 3% and 5% Al content. The AFM result shows that smoothness of the coating surface decreases with increase in doping concentration [22], [23].

Fig.5 (a-d) represents the elemental compositions of prepared samples using EDS. It proves the presence of Zinc and Oxygen in pure ZnO thin film and also the incorporation of Al in ZnO thin films. The insert in figure 4 gives the ratio of elements present in the film. The silicon (Si) peak present in the EDS is originated from the glass substrate. EDS also confirms that Al atomic percent increases from 0.91 to 3.08 with the increase in the doping content.

3.3 Optical Properties

Fig. 6 illustrates the absorption spectram of pristine and Al doped ZnO thin films. The absorption spectrum clearly indicates hyperchromic effect with increase in Al doping. Films show a broad absorption in the ultraviolet region from 300nm - 378nm. The absorption edge was shifted to the lower energy side for Aluminium doped ZnO such similar results were seen in Cd doped ZnO thin films [24]. The material has higher optical property with the presence of Al and thereby, the absorption band edge increases from 366.67 nm for pure ZnO to 371.89 nm for 5% Al doped ZnO. The absorption spectra indicates that

maximum absorption for 5% Al. This might be due to the doping of Al that affects the density of unsaturated bonds making the deviation of local states within the bandgap. Fig.7 represents the relation between $(\alpha h\upsilon)^2$ and $(h\upsilon)$ of the prepared ZnO film with different Al content and the insert denotes bandgap attained by projecting the linear part of the graph and the bandgaps are 3.15eV, 3.12eV, 3.10eV and 3.06eV for pure, 1%, 3% and 5% Al doped ZnO thin films correspondingly**.** The bandgap decreases with the doping of Al content and is explained in terms of stress relaxation mechanism. Such type of red-shift has been reported by Mohanty et al [25]. This suggests the opening of defect states within the bandgap and it can be interpreted due to merging of impurity band into the conduction band, thus shrinking the bandgap. The photoluminescence spectra with an excitation wavelength of 325nm of Al doped ZnO is shown in fig.8. It clearly indicates that the films created a narrow ultraviolet (UV) emission peak and a green emission band. The figure clearly shows a UV peak at approximately 381 nm which is due to ZnO intrinsic emission produced through the recombination of free excitons [26] and a deep-level emission at 450–550 nm is due to zinc interstitial defects and oxygen vacancies [27].

Fig. 9 shows the Antibacterial Assessment of pure and Al doped ZnO. The Al doped ZnO showed significant results than that of undoped ZnO. 5% Al doped ZnO has the maximum zone inhibition of about 25 mm against E.coli and 3% Al doped ZnO has the maximum zone of inhibition of about 21 mm against S.aureus. It is because of the hard bonding of the ZnO elements over the bacteria's external cell membrane. Since then, ZnO particles start to discharge oxygen species into the bacteria that suppress the development of cell which results in the alteration and leakage of the cell and makes the cell to death [28]. The zone of inhibition clearly shows the method of the biocidal activity of the Aluminium doped ZnO that obliterates the external wall of the bacteria and promotes death [29]. The antibacterial effect of Al doped zinc oxide was superior on E.Coli than other strain. This is because the thickness of the cell wall is thin for gram negative bacteria.

Antifungal activity against Aspergillus niger on pure and Al doped ZnO is shown in Fig.10. The maximum zone of inhibition after four days of incubation for pure ZnO, 1%, 3% and 5% Al was found to be 18mm, 10mm, 10mm and 17mm respectively. Both doped and undoped ZnO shows significant antifungal activity. The ZnO particles inhibit the development of Aspergillus niger by affecting the cellular function which leads to the deformation in fungal hyphae [30]. The creation of reactive oxygen species (ROS) is responsible for the increase in the permeability of the cell membrane which enables the cell death.

4. Conclusion

SILAR method is utilized to prepare pure and Al doped ZnO thin films and the films were annealed at 250^{o}C. XRD result reveals that every prepared film is having hexagonal wurtzite arrangement and the outcomes are well matched with the standard JCPDS data (card no. 36-1451). Aluminium doping in ZnO influence the crystallite size by decreasing it sharply. FESEM images reveal spherical morphologies for pure ZnO thin film and hexagonal faced rod like structure for Al doped ZnO thin films. AFM study reveals that RMS values increases with the Al concentration. Incorporation of Al was confirmed from elemental analysis using EDS. In the optical study, the shift towards higher wavelength of the absorption edge was

noticed. The bandgap of ZnO was found to decreases with increase in the Al doping concentration. PL spectrum shows the existence of near band emission and deep level emission. The antibacterial and antifungal results clearly shows that pure and Al doped ZnO has very good antimicrobial effect on microorganisms.

Declarations

Declarations: Not Applicable

Conflict of Interest: None

References

1. R. West, Solid State Chemistry, 2nd edn. (John Wiley & Sons, 1999)
2. Fatemeh Dabir, Hamid Esfahani, Fatemeh Bakhtiargonbadi, Zahra Khodadadi, Journal of Sol-Gel Science and Technology, (2020) https://doi.org/10.1016/j.jallcom.2012.11.057
3. Jun Sawai, Emiko Kawada, Fumio Kanou, Hideo Igarashi, Atsushi Hashimoto, Takao Kokugan, Masaru Shimizu, Journal of Chemical Engineering of Japan, (1996) https://doi.org/10.1252/jcej.29.627
4. Andrea Gracia Cuevas, Kryssa Balangcod, Teodora Balangcod, Alladin Jasmin, Procedia Engineering, (2013) https://doi.org/10.1016/j.proeng.2013.12.218
5. Srinivasan, J. C. Kannan and S. Satheeskumar, International Journal of PharmTech Research, **7** (2), 287-290 (2014-2015).
6. P Anitha, S R Madhan Shankar, Em Rajesh, Namitha Purushothaman, A Anulakshmi, R Rajendran, Bionano Frontier, **7** (1), 16-22 (2014).
7. S. Shinde, A.P. Korade, C.H. Bhosale, K.Y. Rajpure, Journal of Alloys and Compounds, (2013) https://doi.org/10.1016/j.jallcom.2012.11.057
8. Wahab, A. Mishra, S. Yun, I.H Hwang, J. Mussarat, A.A. Al-khedhairy, Young-soon Kim, H. Shin, Biomass and Bioenergy, (2012) https://doi.org/10.1016/j.biombioe.2012.01.005
9. Panigrahi, B. Behera, I. Mohanty, U. Subudhi, B.B. Nayak, B.S. Acharya Applied Surface Science, (2011) https://doi.org/10.1016/j.apsusc.2011.08.056
10. Amornpitoksuk, S. Suwanboon, S. Sangkanu, A. Sukhoom, J. Wudtipan, K.Srijan, S. Kaewtaro, Powder Technology, (2011) https://doi.org/10.1016/j.powtec.2011.06.028
11. K, Mugwang'a, P.K. Karimi, W.K. Njoroge, O. Omayio, Applications, Journal of Fundamentals of Renewable Energy and Applications, **5** (4), (2015).
12. Sara Marouf, Abdelkrim Beniaiche, Hocine Guessas, Amor Azizi, Materials Research, (2017) https://doi.org/10.1590/1980-5373-mr-2015-0751
13. R. Alfaro Cruz, O. Ceballos-Sanchez, E. Luévano-Hipólito, L. M. Torres-Martínez, International Journal of Hydrogen Energy, (2018) https://doi.org/10.1016/j.ijhydene.2018.04.054

14. Kathalingam, N. Ambika, M. R. Kim, J. Elanchezhiyan, Y. S. Chae, J. K. Rhee, Materials Science-Poland, **28** (2), (2010).
15. Lehraki, M.S. Aida, S. Abed, N. Attaf, A. Attaf, M. Poulain, Current Applied Physics, (2012) https://doi.org/10.1016/j.cap.2012.03.012
16. G.Valle, P. Hammer, S.H. Pulcinelli, C.V.Santilli, Journal of the European Ceramic Society, (2004) https://doi.org/10.1016/S0955-2219(03)00597-1
17. Assumpta C. Nwanya, P.R. Deshmukh, Rose U. Osuji, Malik Maaza, C.D. Lokhande, Fabian I. Ezema, Sensors and Actuators B: Chemical, (2015) https://doi.org/10.1016/j.snb.2014.09.111
18. Schuler, M. A. Aegerter, Thin Solid Films, (1991) https://doi.org/10.1016/S0040-6090(99)00211-4
19. Bandyopadhyay, G. K. Paul, R. Roy, S.K. Sen, S. Sen, Materials Chemistry and Physics, (2002) https://doi.org/10.1016/S0254-0584(01)00402-3
20. Caglar, M. Cagla, S. Ilican, Current Applied Physics, (2012) https://doi.org/10.1016/j.cap.2011.12.017
21. Reza Mahdavi, S. Siamak Ashraf Talesh, Advanced Powder Technology, (2017) https://doi.org/10.1016/j.apt.2017.03.014
22. Manjeet Kumar, Bikmramjeet Singh, Pankaj Yadav, Vishwa Bhatt, Manoj Kumar, Kulwinder Singh, A.C. Abhyankar, Akshay Kumar, Ju-Hyung Yun, Ceramics International, (2017) https://doi.org/10.1016/j.ceramint.2016.11.191
23. Deniz Kadir Takci, Ebru Senadim Tuzemen, Kamuran Kara, Sadi Yilmaz, Ramazan Esen,Ozge Baglayan, Journal of Materials Science: Materials in Electronics, (2014) https://doi.org/10.1007/s10854-014-1843-0
24. K. Shan, G.X. Liu, W.J. Lee, B.C. Shin, Journal of Crystal Growth, (2006) https://doi.org/10.1016/j.jcrysgro.2006.03.036
25. Bhaskar Chandra Mohanty, YeonHwa Jo, DeukHoYeon, Ik Jin Choi, Yong Soo Cho, Applied Physics Letters, (2009) https://doi.org/10.1063/1.3202399
26. W. Wang, Y. H. Yang, G. W. Yang, Journal of Physical Chemistry C, (2009) https://doi.org/10.1021/jp906924w
27. Bingqiang Cao, WeipingCai, HaiboZeng, Applied Physics Letters, (2006) https://doi.org/10.1063/1.2195694
28. Nuengruethai Ekthammathat, Somchai Thongtem, Titipun Thongtem, Anukorn Phuruangrat, Powder Technology, (2014) https://doi.org/10.1016/j.powtec.2014.01.010.
29. Manoharan, G. Pavithra, M. Bououdina, S. Dhanapandian, P. Dhamodharan, Applied Nanoscience, (2016) https://doi.org/10.1007/s13204-015-0493-8.
30. Lili He, Yang Liu, Azlin Mustapha and Mengshi Lin, Microbiological Research, (2011) https://doi.org/10.1016/j.micres.2010.03.003.

Figures

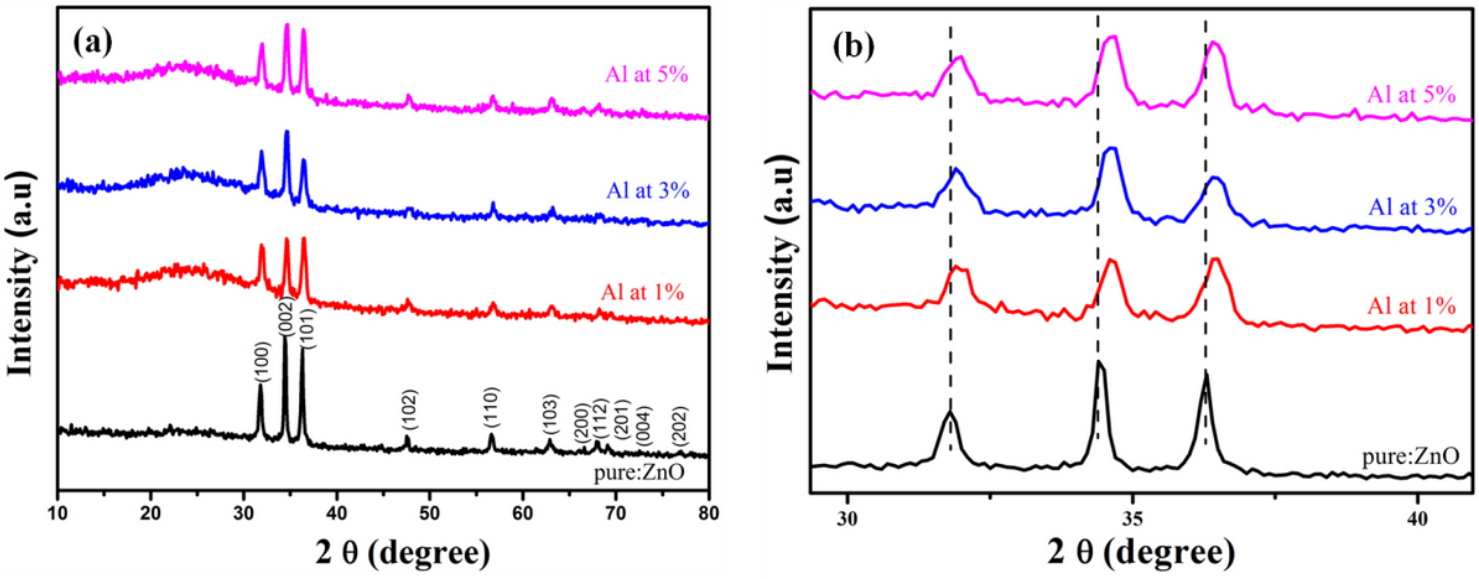

Figure 1

X-ray diffraction pattern of pure and Al doped ZnO thin films

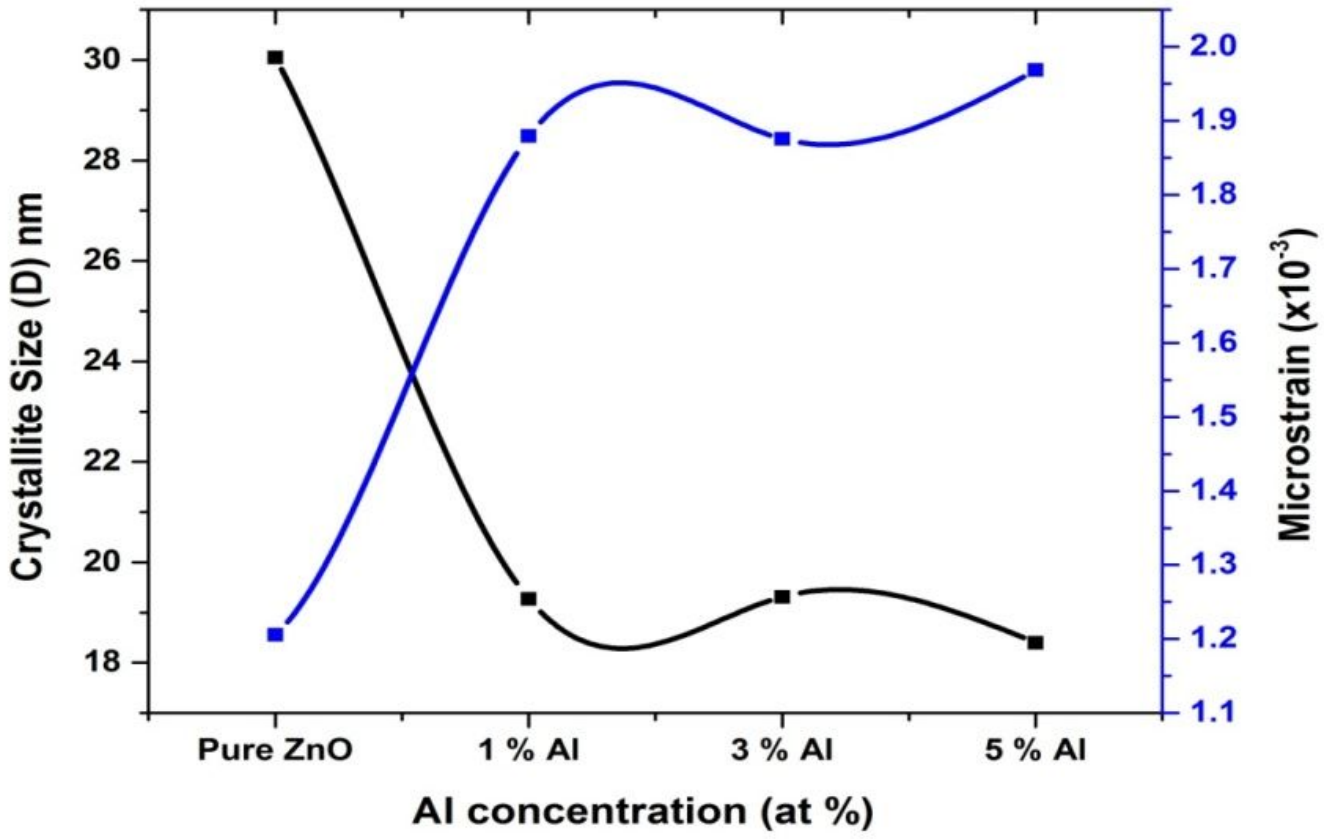

Figure 2

Al doping effect on crystallite size and microstrain

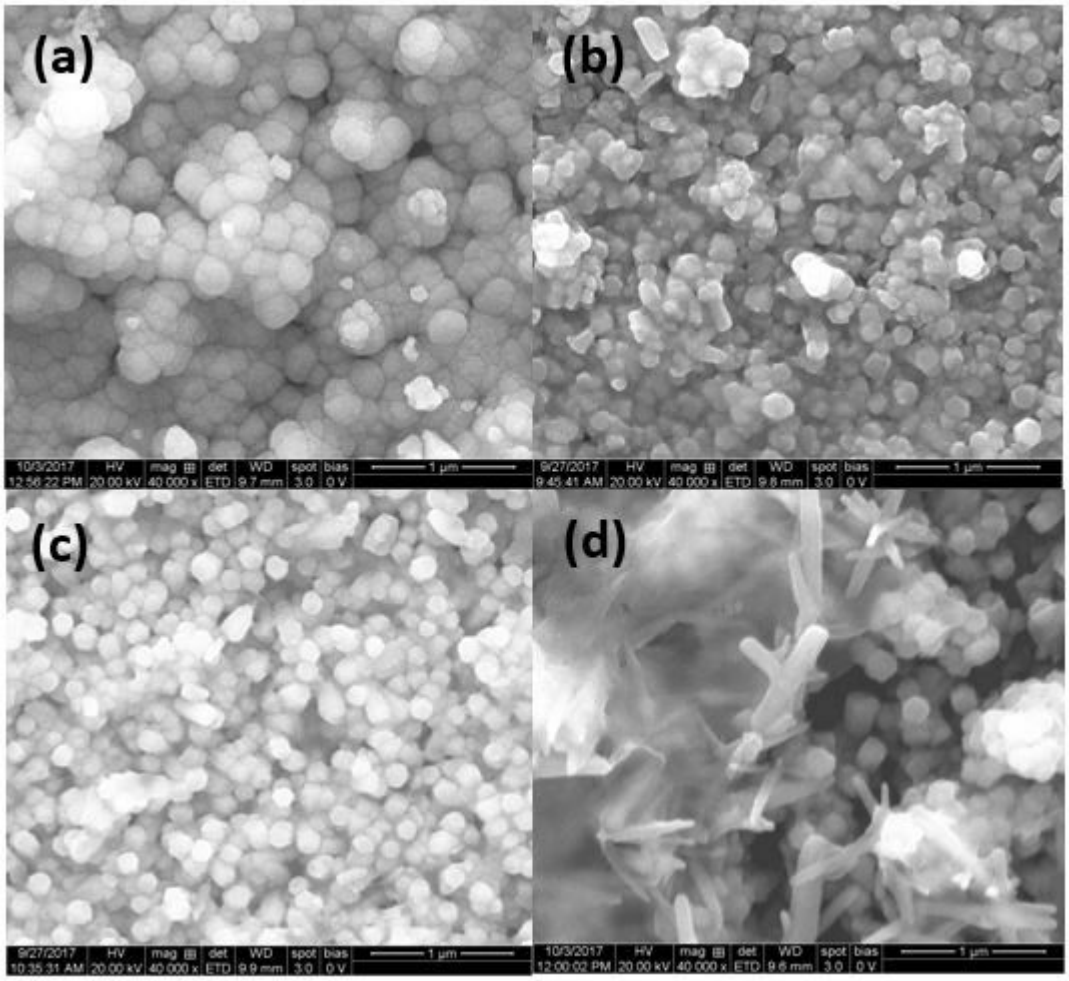

Figure 3

FESEM Images of (a) pure, (b) 1% Al, (c) 3% Al and (d) 5% Al doped ZnO thin films

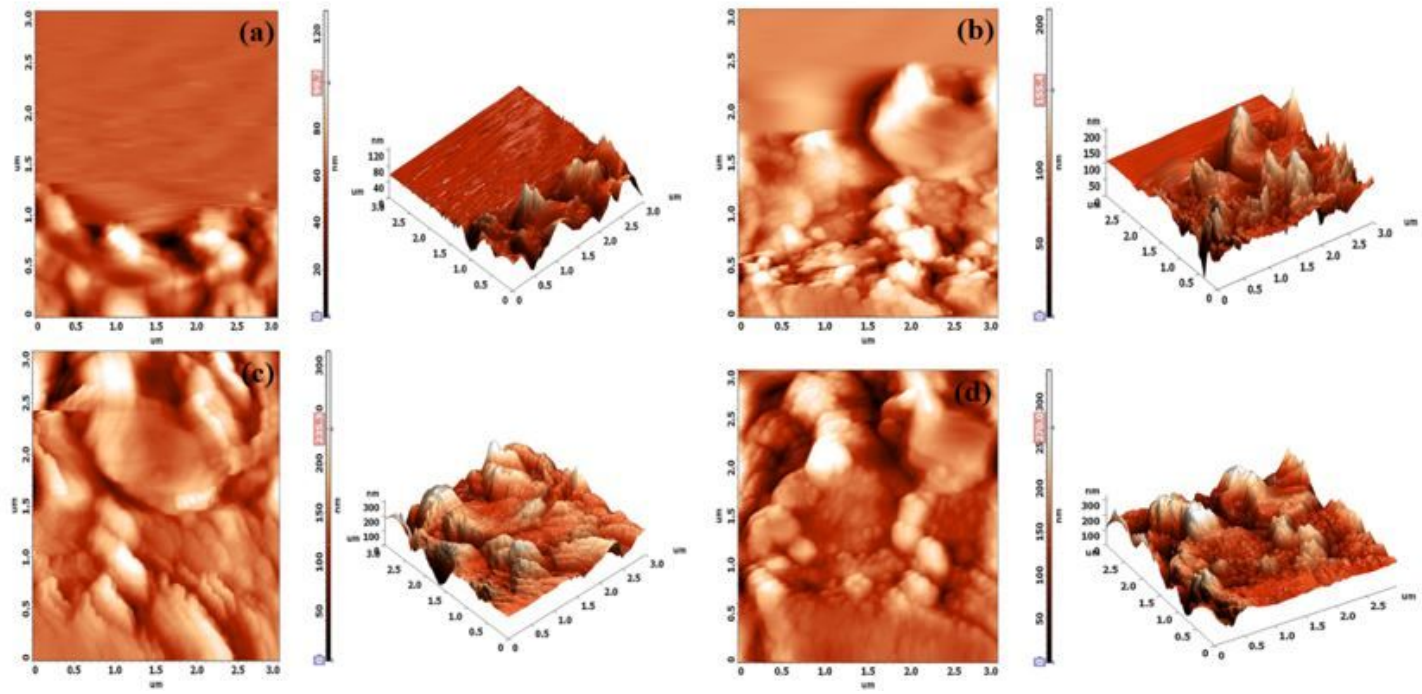

Figure 4

AFM Images of (a) pure, (b) 1% Al, (c) 3% Al and (d) 5% Al doped ZnO thin films

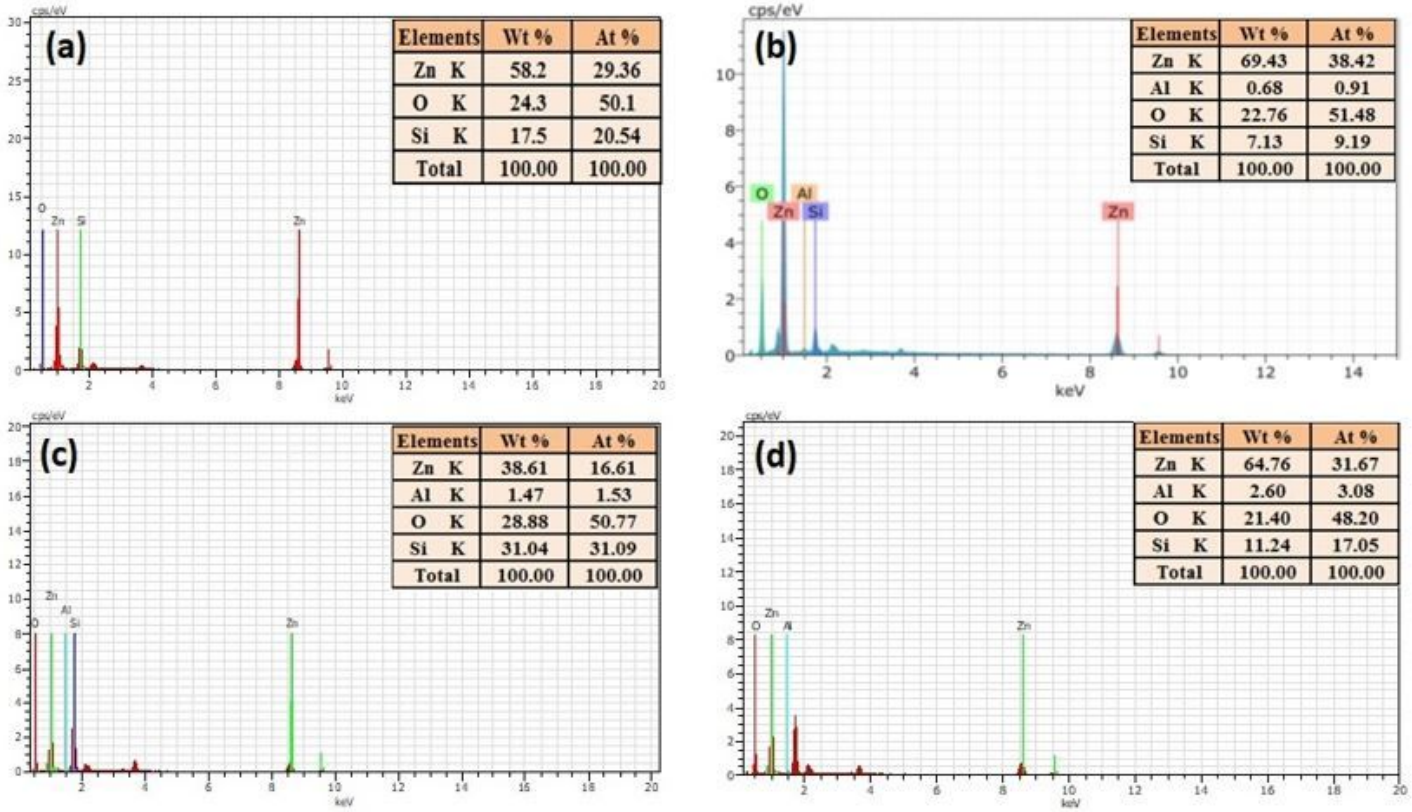

Figure 5

EDS Images of (a) pure, (b) 1% Al, (c) 3% Al and (d) 5% Al doped ZnO thin films

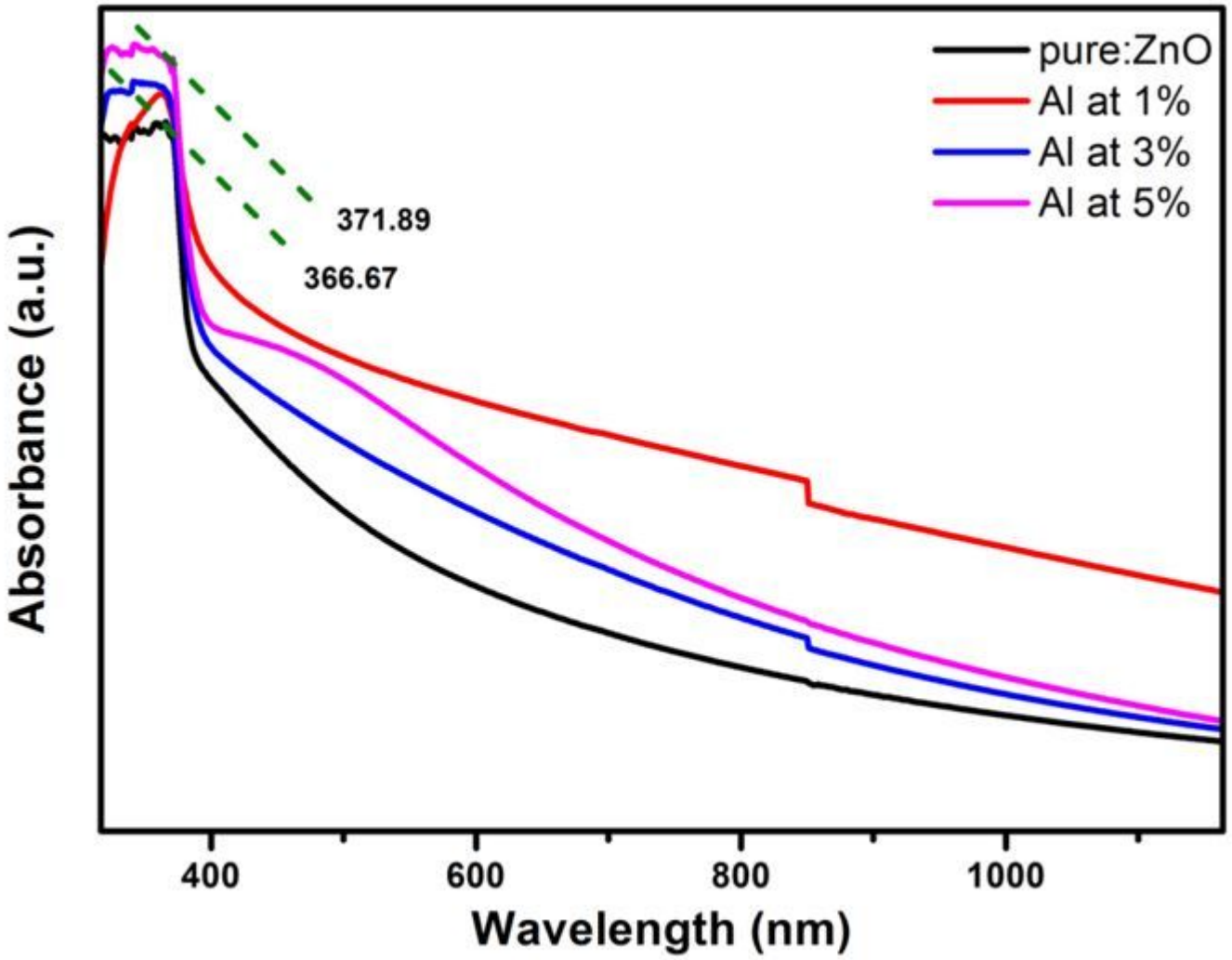

Figure 6

Absorption spectrum of pure and Al doped ZnO thin films

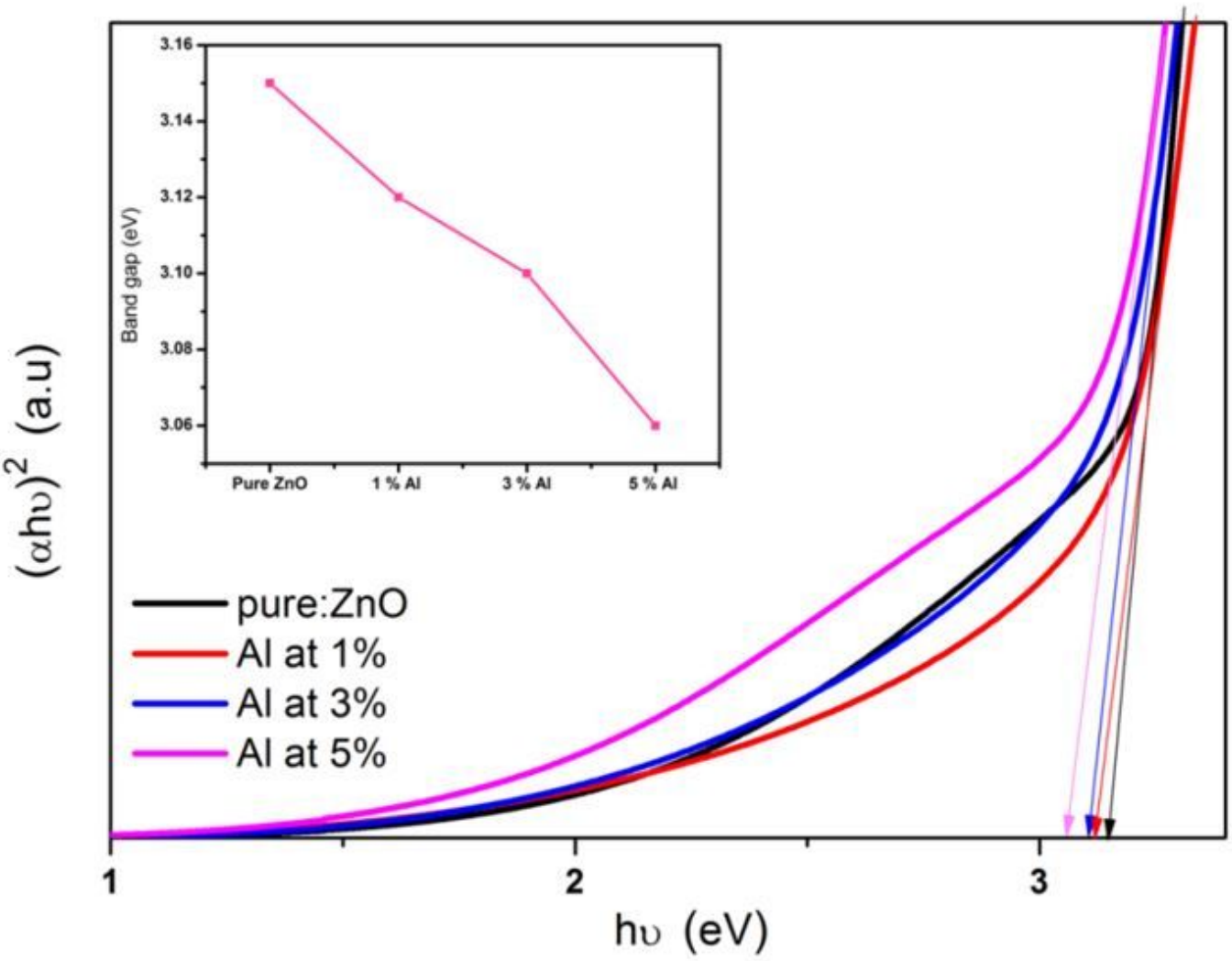

Figure 7

Plot of (αhυ)2 vs photon energy (hυ) of ZnO film with different Al concentration.

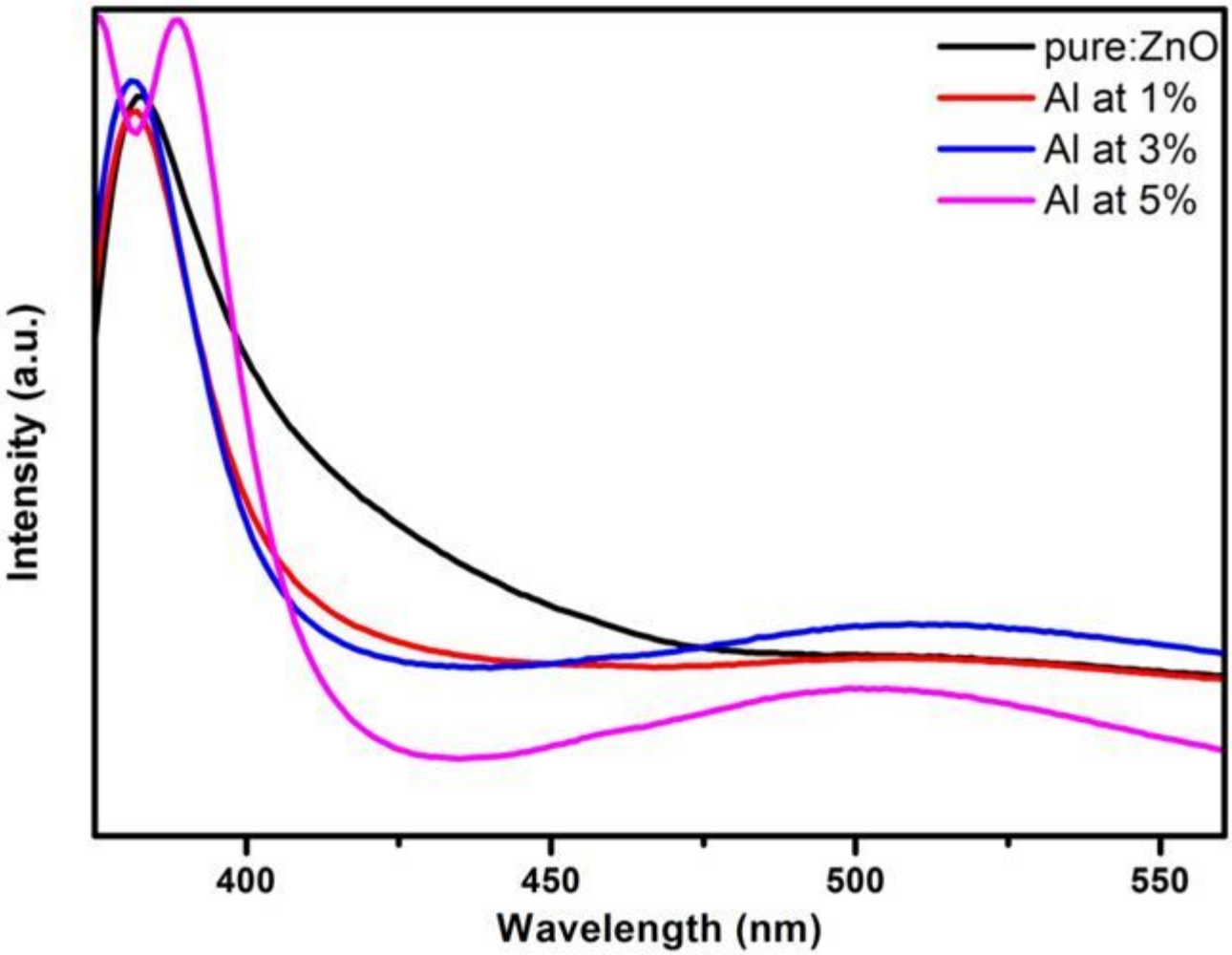

Figure 8

PL Spectrum of Pure and Al doped ZnO Thin Films.

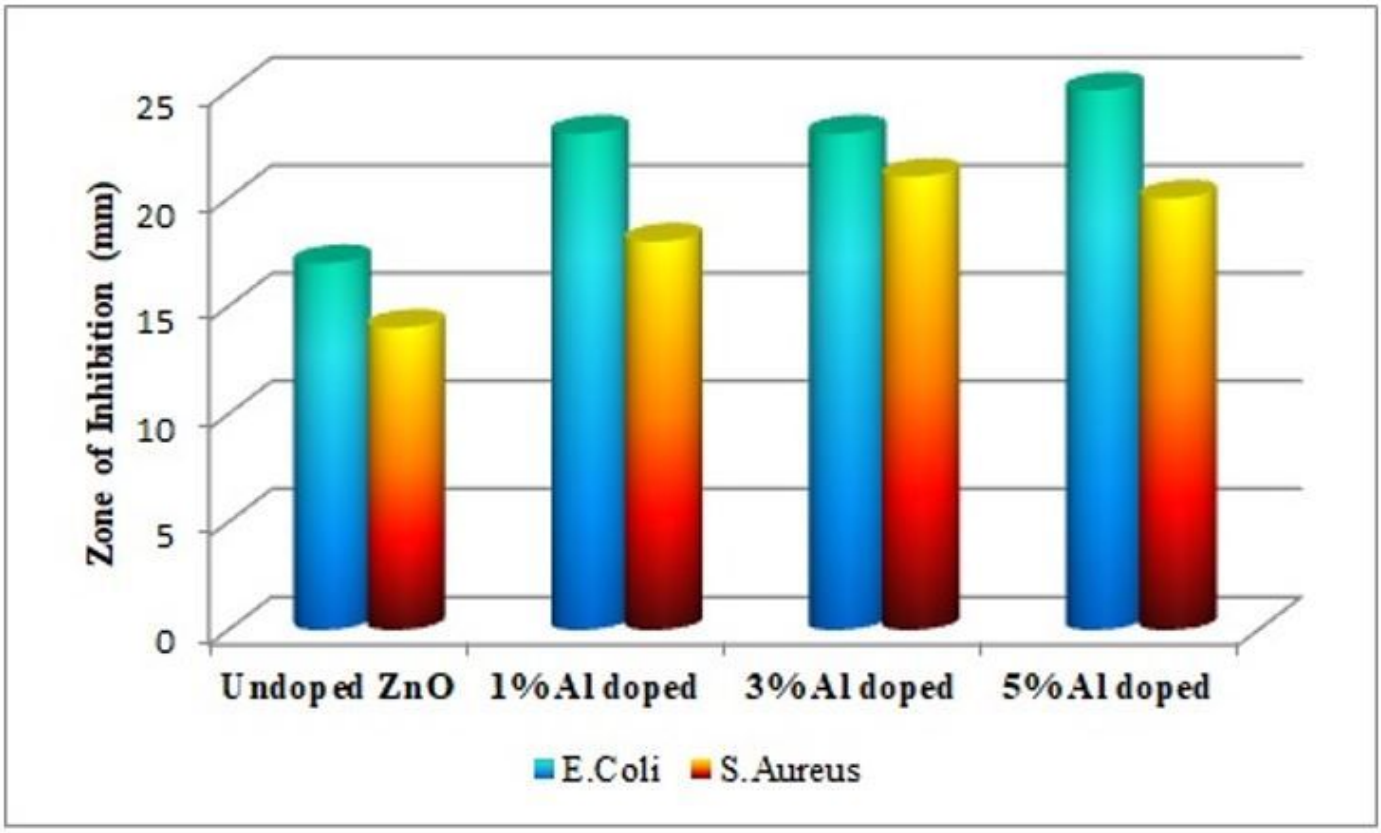

Figure 9

Antibacterial activity of pure and Al doped ZnO

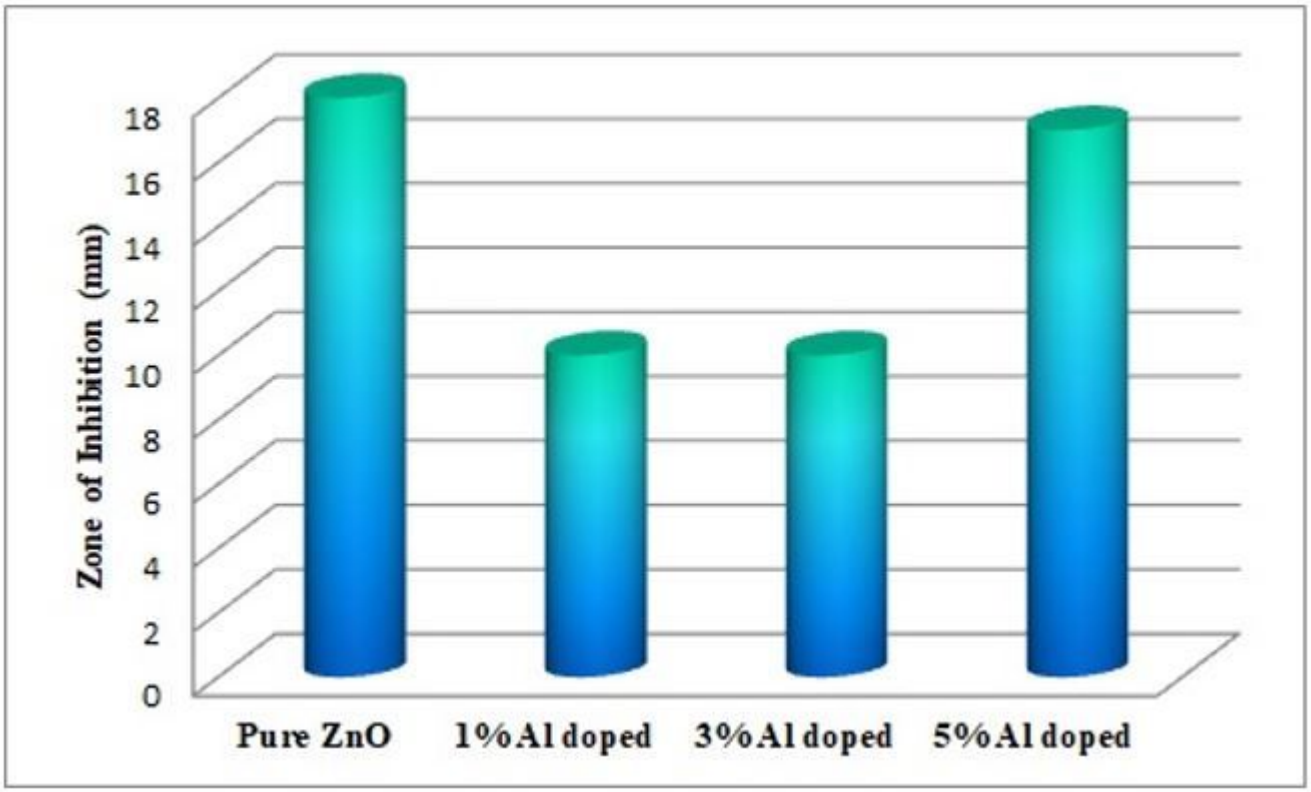

Figure 10

Antifungal activity of pure and Al doped ZnO